

## Nucleophile Specificity in Anthranilate Synthase, Aminodeoxychorismate Synthase, Isochorismate Synthase, and Salicylate Synthase

Kristin T. Ziebart and Michael D. Toney\*

Department of Chemistry, University of California, Davis, California 95616

Received January 7, 2010; Revised Manuscript Received February 15, 2010

**ABSTRACT:** Anthranilate synthase (AS), aminodeoxychorismate synthase (ADCS), isochorismate synthase (IS), and salicylate synthase (SS) are structurally homologous chorismate-utilizing enzymes that carry out the first committed step in the formation of tryptophan, folate, and the siderophores enterobactin and mycobactin, respectively. Each enzyme catalyzes a nucleophilic substitution reaction, but IS and SS are uniquely able to employ water as a nucleophile. Lys147 has been proposed to be the catalytic base that activates water for nucleophilic attack in IS and SS reactions; in AS and ADCS, glutamine occupies the analogous position. To probe the role of Lys147 as a catalytic base, the K147Q IS, K147Q SS, Q147K AS, and Q147K ADCS mutants were prepared and enzyme reactions were analyzed by high-performance liquid chromatography. Q147K AS employs water as a nucleophile to a small extent, and the cognate activities of K147Q IS and K147Q SS were reduced ~25- and ~50-fold, respectively. Therefore, Lys147 is not solely responsible for activation of water as a nucleophile. Additional factors that contribute to water activation are proposed. A change in substrate preference for K147Q SS pyruvate lyase activity indicates Lys147 partially controls SS reaction specificity. Finally, we demonstrate that AS, ADCS, IS, and SS do not possess chorismate mutase promiscuous activity, contrary to several previous reports.

The shikimate pathway occurs in bacteria, plants, fungi, and apicomplexan parasites (1, 2). Starting with phosphoenolpyruvate and D-erythrose 4-phosphate and ending with chorismate, it enables de novo biosynthesis of carbocyclic aromatic compounds. Chorismate is the common precursor of a variety of essential metabolites such as phenylalanine, tyrosine, tryptophan, folate, siderophores, menaquinones, and others. Production of several phenazines, known to impart virulence and competitive fitness to the opportunistic pathogen *Pseudomonas aeruginosa*, also begins with chorismate (3). The central role of chorismate-utilizing enzymes in the survival of these organisms and their absence in humans make them attractive targets for herbicides and antimicrobial drugs.

Figure 1 depicts seven branch points in chorismate metabolism. With the exception of chorismate lyase (CL)<sup>1</sup> and chorismate mutase (CM), these enzymes are structurally homologous. X-ray crystal structures of anthranilate synthase (AS), aminodeoxychorismate synthase (ADCS), isochorismate synthase (IS), and salicylate synthase (SS) reveal them to be highly similar proteins with conserved active sites (4–11). These similarities, along with an abundance of biochemical evidence (12, 13), led He et al. to propose a common mechanism in which catalysis begins with nucleophilic attack at C2 of chorismate, concomitant with displacement of the C4 hydroxyl group in an S<sub>N</sub>2'' reaction (14).

In this mechanism, IS and SS employ water as a nucleophile, yet AS and ADCS do not, despite its abundance (Figure 2). Instead, AS and ADCS utilize ammonia that is provided from companion glutamine amidotransferases TrpG and PabA, respectively. ADCS is unique in its use of an active site lysine (K213) as the initial nucleophile attacking at C2; in a second S<sub>N</sub>2'' reaction, nucleophilic attack by ammonia at C4 of the covalent intermediate leads to the final product (14–16). ADCS and IS release the nucleophile-substituted chorismate as the product, while AS and SS proceed further by eliminating pyruvate and releasing the resulting aromatic product.

In AS and ADCS, the companion amidotransferase subunit delivers ammonia directly to the active site where chorismate binds and undergoes nucleophilic substitution. An ammonia tunnel is believed to exist between the amidotransferase and chorismate-aminating active sites; this is a common mechanism for avoiding free intracellular ammonia (17, 18). In the absence of L-glutamine and an amidotransferase subunit, AS and ADCS can employ (NH<sub>4</sub>)<sub>2</sub>SO<sub>4</sub> as an ammonia source (14, 19). Although IS and SS lack a source of ammonia in vivo, each will accept it as a nucleophile in vitro to form aminodeoxyisochorismate (ADIC) and anthranilate, respectively (vide infra and ref 16). Since intracellular ammonia concentrations are generally low, IS and SS apparently have not needed to develop a means of discriminating against this nucleophile. However, since water is a poor nucleophile and is not employed by AS and ADCS, water activation must exclusively exist in IS and SS to explain the observed nucleophile specificity among these enzymes.

Sequence alignments indicate a conserved active site lysine residue exists in all IS and SS sequences (9). A glutamine residue occupies the analogous position in all ADCS and AS sequences. Recent crystal structures of MenF, a menaquinone-specific IS, and Irp9, the SS from *Yersinia enterocolitica*, reveal this lysine to

\*To whom correspondence should be addressed. E-mail: mdtoney@ucdavis.edu. Telephone: (530) 754-5282. Fax: (530) 752-8995.

<sup>1</sup>Abbreviations: CL, chorismate lyase; CM, chorismate mutase; AS, anthranilate synthase; ADCS, 4-amino-4-deoxychorismate synthase; IS, isochorismate synthase; SS, salicylate synthase; PD, prephenate dehydratase; ADCL, 4-amino-4-deoxychorismate lyase; MenF, menaquinone-specific IS; Irp9, SS from *Yersinia enterocolitica*; MbtI, SS from *Mycobacterium tuberculosis*; ADIC, 2-amino-4-deoxyisochorismate; ADC, 4-amino-4-deoxychorismate; PHB, *p*-hydroxybenzoate; HPLC, high-performance liquid chromatography.

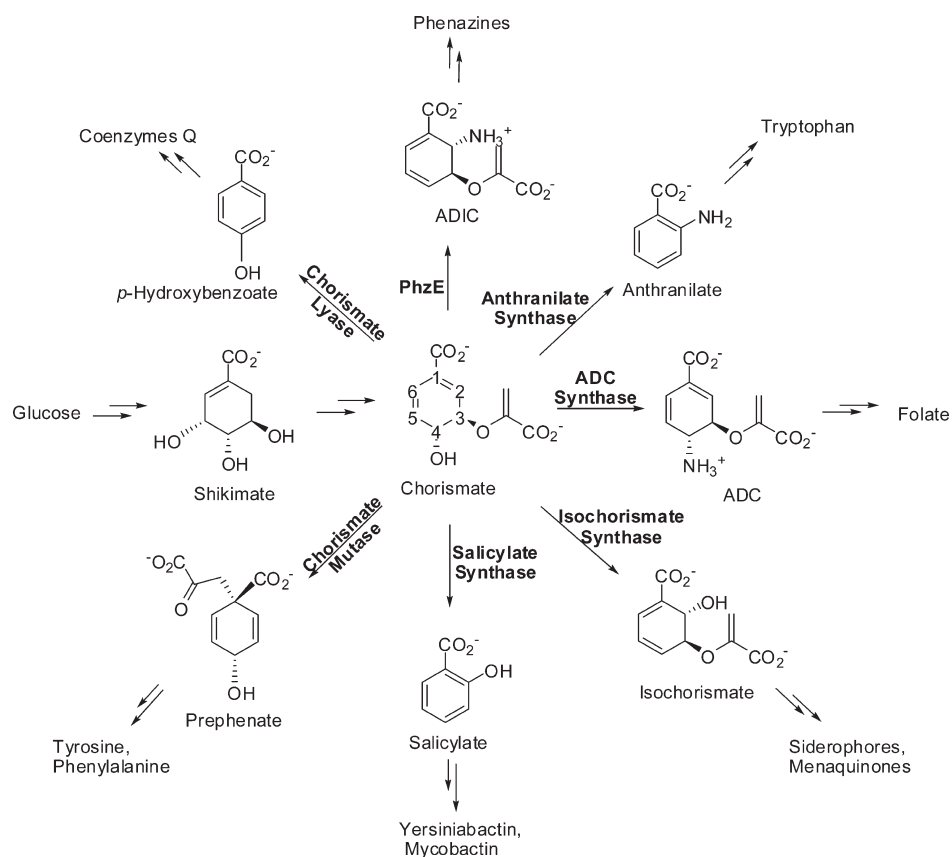


FIGURE 1: Chorismate is a central branch point compound in plant, bacterial, fungal, and apicomplexan parasite metabolism. With the exception of chorismate mutase and chorismate lyase, the enzymes shown are structurally similar. Each enzyme catalyzes the first committed step toward biosynthesis of a carbocyclic aromatic metabolite essential for cell survival and/or virulence.

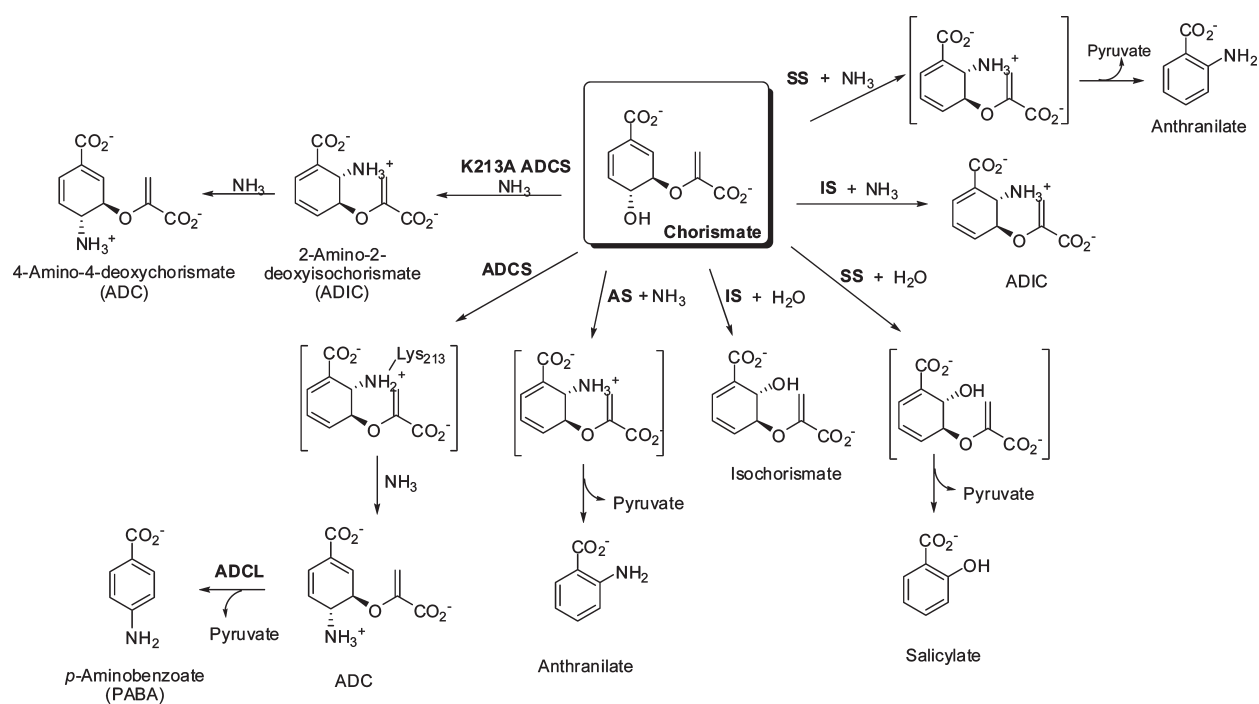


FIGURE 2: Chorismate undergoes nucleophilic attack at C2 by ammonia (AS), Lys213 (ADCS), or water (IS and SS). SS and IS employ  $\text{NH}_3$  as a nucleophile if supplied exogenously, but AS and ADCS are unable to activate water as a nucleophile. K213A ADCS activity is rescued by  $(\text{NH}_4)_2\text{SO}_4$ .

be well-positioned between an ordered water molecule and C2 of chorismate (4, 11). On the basis of the available structural evidence and the fact that a K147A IS mutant was inactive,

Kolappan et al. proposed Lys147 to be the general base catalyst that activates water for nucleophilic attack in IS and SS reactions (9).

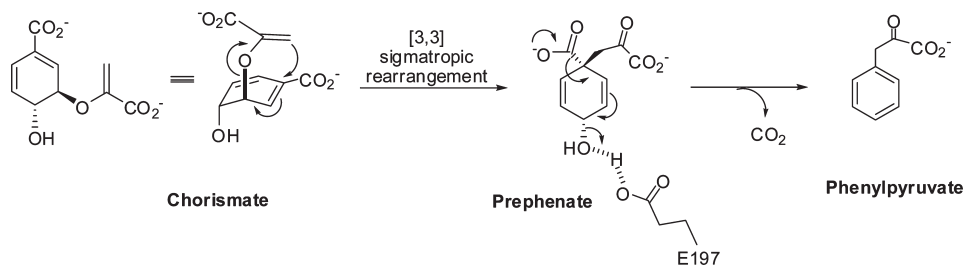


FIGURE 3: Abell and co-workers' proposed mechanism for promiscuous formation of phenylpyruvate by AS and SS (19). The diaxial conformation of chorismate undergoes pericyclic rearrangement to form prephenate, followed by decarboxylation and general acid-assisted loss of water. Glu197 is conserved in all AS and SS sequences. Data presented here demonstrate that these reactions are not catalyzed by AS and SS.

Seeking to provide additional biochemical insight into the catalytic role of Lys147, we mutated it here to a glutamine in MbtI (the SS from *Mycobacterium tuberculosis*) and EntC (the enterobactin-specific IS); the corresponding glutamine to lysine mutants of the ammonia-utilizing AS and ADCS were also prepared. Kerbarh et al. performed similar experiments with AS and Irp9 SS (20). In that study, enzyme-catalyzed reactions were conducted at pH 7 and product mixtures were analyzed by  $^1\text{H}$  NMR; a reciprocal switch in nucleophile specificity was not observed. The major result of Kerbarh et al. was that AS and Irp9 mutants apparently catalyze formation of phenylpyruvate. As illustrated in Figure 3, Kerbarh et al. proposed that SS, K147Q SS, and Q147K AS catalyze two successive promiscuous reactions: pericyclic rearrangement of chorismate to form prephenate, followed by decarboxylation and loss of water to form phenylpyruvate.

This work substantially builds upon previous results and addresses more thoroughly the issue of nucleophile specificity in the following ways. (1) Four enzymes, AS, ADCS, IS, and SS, are under study instead of just two. (2) Reaction mixtures are analyzed by HPLC, which affords a detection limit of reaction products lower than that for  $^1\text{H}$  NMR. (3)  $(\text{NH}_4)_2\text{SO}_4$ -dependent reactions are conducted at pH 8 instead of pH 7, thus increasing the concentration of  $\text{NH}_3$  10-fold. (4) The source of promiscuous chorismate mutase and prephenate dehydratase activities is explained.

## EXPERIMENTAL PROCEDURES

**Materials.** All chemical reagents were purchased from Sigma-Aldrich and used without further purification. Lysozyme was purchased from Sigma. Glutamate dehydrogenase (GDH) was purchased from Calzyme. Lactate dehydrogenase (LDH) and DNaseI were purchased from Roche. Chorismate was prepared according to a literature procedure (21).

**Enzyme Preparation.** The preparation of plasmid constructs bearing the genes *pabA*, *pabB*, and *entC* was described previously (14, 16). Overexpression and purification of the proteins encoded by these three genes, PabA, ADCS, and IS, respectively, were conducted according to literature procedures (14, 16). Protein yields were as follows: 83 mg of PabA/15 g of cell paste, 330 mg of ADCS/20 g of cell paste, and 213 mg of IS/42 g of cell paste.

Mutations were introduced using Stratagene's QuikChange site-directed mutagenesis kit. Construction of the ADCS double mutant (K274A/Q211K) used pET28a-*pabB*-K274A as the template strand (note that Q211 is the residue analogous to K147, and K274 is analogous to A213 in the EntC IS sequence).<sup>2</sup> The preparation of K274A ADCS was described previously (14). The

K274A/Q211K mutagenic primers were 5'-CGGTGATTGC-TATAAGGTGAATCTCGCC (forward) and 5'-GGCGAGATTACCTTATAGCAATCACCG (reverse). K274A/Q211K ADCS was expressed and purified in a manner similar to that of wild-type (WT) ADCS. The protein yield was 190 mg/23 g of cell paste.

For K147Q IS, the mutation was created in the pET28a-*entC* construct using the following mutagenic primers: 5'-GCCG-CAGGTCGACCAAGTGGTGTG (forward) and 5'-CAACACCACCTTGGTCGACCTGCGGC (reverse). K147Q IS was overexpressed and purified in a manner similar to that of WT IS. The protein yield was 182 mg/26 g of cell paste.

Open reading frame Rv2386c of *M. tuberculosis* genomic DNA encodes MbtI, a protein identified as a salicylate synthase (10). The *E. coli* codon-optimized synthetic gene (procured from Mr. Gene) was subcloned into a pET28a expression vector (Novagen) using NdeI and BamHI restriction sites. After *E. coli* BL21(DE3) cells harboring a pET28a-*mbtI* plasmid had been grown in LB medium at 37 °C to OD<sub>600</sub> of 2, SS overexpression proceeded for 7 h at 30 °C after induction with 0.5 mM IPTG. Cells were harvested by centrifugation and resuspended in lysis buffer [20 mM  $\text{Na}_2\text{HPO}_4$ , 500 mM NaCl, 10 mM imidazole (pH 7.4), 0.5 mg/mL lysozyme, and 0.2 unit/mL DNase I] prior to disruption by sonication. Cell debris was pelleted by centrifugation at 14000 rpm for 45 min. The supernatant was incubated at 4 °C for 45 min with Chelating Sepharose Fast Flow resin (Pharmacia) that had been charged with  $\text{Ni}^{2+}$ . The resin was loaded into a column and washed with 10 column volumes of starting buffer [20 mM  $\text{Na}_2\text{HPO}_4$ , 500 mM NaCl, and 10 mM imidazole (pH 7.4)]. Protein was eluted with a linear gradient of 500 mL from 10 to 300 mM imidazole in starting buffer. The purest fractions, as judged by SDS-PAGE analysis, were concentrated by ultrafiltration and dialyzed against 20 mM KP<sub>i</sub> (pH 7.5), 50 mM KCl, and 1 mM DTT. Purified enzyme was flash-frozen and stored at -80 °C. Protein concentrations were measured with the Lowry protein assay kit (Bio-Rad) using IgG as a standard. The protein yield was 25 mg/33 g of cell paste.

For K205Q SS, the mutation was created in the pET28a-*mbtI* construct using the following mutagenic primers: 5'-CTGGT-CGTTACCACCAAGTTATTCTGTCCC (forward) and 5'-GGGACAGAATAACTTGGTGGTAACGACCAG (reverse). K205Q SS was overexpressed and purified in a manner similar to that of WT SS (note that K205 is analogous to K147 in the EntC IS sequence). The protein yield was 40 mg/31 g of cell paste.

A small portion of each His-tagged protein that had been purified by nickel affinity chromatography was subjected to a second purification by anion exchange. Protein, which had been stored in 20 mM KP<sub>i</sub> (pH 7.5), 50 mM KCl, and 1 mM DTT at

<sup>2</sup>The numbering used throughout is based on the EntC protein from *Escherichia coli*.

−80 °C, was thawed and loaded onto a 50 mL Q-Sepharose Fast Flow (Pharmacia) column that had been equilibrated with start buffer [10 mM triethanolamine hydrochloride (TEA-HCl) (pH 7.8), 10 mM mercaptoethanol, 5 mM MgCl<sub>2</sub>, and 1 mM EDTA]. Protein was eluted with a linear gradient of 500 mL from 0 to 300 mM KCl in start buffer. The purest fractions, as judged by SDS-PAGE, were concentrated by ultrafiltration and dialyzed against 20 mM KP<sub>i</sub> (pH 7.5), 50 mM KCl, and 1 mM DTT. The purified enzyme was flash-frozen and stored at −80 °C. The activity of each doubly purified protein was the same as that measured for the singly purified protein.

The plasmid construct bearing the genes for the partial complex of anthranilate synthase (TrpE<sub>2</sub>-TrpG<sub>2</sub>) was a gift from R. Bauerle (University of Virginia, Charlottesville, VA). Partial complex anthranilate synthase (AS) from *Salmonella typhimurium* consists of a TrpE<sub>2</sub>-TrpG<sub>2</sub> heterotetramer. Plasmid pSTC25 contains two tandem stop codons engineered into the *trpD* gene, such that only the region encoding amidotransferase activity is expressed; the polypeptide translated from this truncated gene is named TrpG (19).

AS was prepared in the following manner. *E. coli* cells (strain CB694) harboring the pSTC25 construct were grown in LB medium at 37 °C to an OD<sub>600</sub> of 2.5–3. Cells were harvested by centrifugation, resuspended in 10 mM TEA (pH 7.8), 10 mM mercaptoethanol, 5 mM MgCl<sub>2</sub>, 1 mM EDTA, 0.5 mg/mL lysozyme, and 0.2 unit/mL DNaseI, and then disrupted by sonication. Cell debris was pelleted by centrifugation at 14000 rpm. Ammonium sulfate was added to 23% saturation to the soluble extract; the resulting precipitate was resuspended in a minimum volume of start buffer [10 mM TEA (pH 7.8), 10 mM mercaptoethanol, 5 mM MgCl<sub>2</sub>, and 1 mM EDTA] and loaded onto a 50 mL Q-Sepharose Fast Flow column. Protein was eluted with a linear gradient of 500 mL from 0 to 300 mM KCl in start buffer. The purest fractions, as judged by SDS-PAGE, were concentrated by ultrafiltration and dialyzed against 20 mM KP<sub>i</sub> (pH 7.5), 50 mM KCl, and 1 mM DTT. The purified enzyme was flash-frozen and stored at −80 °C. The protein concentration was measured with the Lowry protein assay kit (Bio-Rad), using IgG as a standard. The yield was 142 mg of purified protein/10 g of cell paste.

Introduction of the Q263K mutation into the *trpE* gene within pSTC25 used the following mutagenic primers: 5'-GGCGAGATATTTAAGGTGGTGCCGTC (forward) and 5'-GACGGCACCACCTTAAATATCTCGCC (reverse) (note that Q263 is the residue analogous to K147 in EntC IS). Q263K AS was overexpressed and purified in a manner similar to that of WT AS. The protein yield was 173 mg/22 g of cell paste.

Lacking a His tag, AS and Q263K AS could not be purified by nickel affinity chromatography. Therefore, these were repurified via hydroxyapatite chromatography. Protein, which had been stored in 20 mM KP<sub>i</sub> (pH 7.5), 50 mM KCl, and 1 mM DTT at −80 °C, was thawed and loaded onto a column containing CHT Ceramic Hydroxyapatite resin (Bio-Rad) that had been equilibrated with start buffer [5 mM sodium phosphate and 150 mM NaCl (pH 6.8)]. Protein was eluted with a linear gradient of 500 mL from 5 to 500 mM sodium phosphate in start buffer. The purest fractions, as judged by SDS-PAGE, were combined and concentrated by ultrafiltration and dialyzed against 20 mM KP<sub>i</sub> (pH 7.5), 50 mM KCl, and 1 mM DTT. Purified enzyme was flash-frozen and stored at −80 °C. The activity of the doubly purified protein was the same as that measured for the singly purified protein.

**Spectrofluorometric AS Activity Assays.** These were performed on a PerkinElmer LS 50B luminescence spectrophotometer at 25 °C. The enzyme activity assay for AS was based on a previously described method (19). The assay directly monitors anthranilate emission at 390 nm using excitation at 313 nm. Reactions were initiated by addition of anthranilate synthase. The standard glutamine-dependent assay contains 100 mM phosphate buffer (pH 7.0), 20 mM L-glutamine, 5 mM MgCl<sub>2</sub>, and 2.2 nM WT AS. The standard NH<sub>4</sub><sup>+</sup>-dependent assay contains 100 mM TEA-HCl (pH 8.0), 100 mM (NH<sub>4</sub>)<sub>2</sub>SO<sub>4</sub>, 5 mM MgCl<sub>2</sub>, and 2.2 nM WT AS. The same assays were used to monitor Q147K AS-catalyzed reactions. The protein concentration of Q147K AS was increased 500 nM to compensate for the decreased activity of the mutant.

**Spectrophotometric Activity Assays.** Kinetic assays were performed on a Kontron Uvikon 930 UV-vis spectrophotometer at 25 °C. Amidotransferase activity was measured in a coupled assay with excess glutamate dehydrogenase (GDH) that was based on a previously described method (22). PabA glutaminase activity was measured while it was in complex with either WT ADCS or K213A/Q147K ADCS. Each 500 μL reaction mixture contained 100 mM TEA-HCl (pH 9.0), 5 mM MgCl<sub>2</sub>, 4 mM 3-acetylpyridine adenine dinucleotide (APAD), 20 units of GDH, 0.5 μM PabA, and 0.75 μM ADCS (same concentration used for both WT and K213A/Q147K reactions). The L-glutamine concentration was varied from 0.1 to 4.0 mM.

The activity of TrpG, measured while in a tetrameric complex with either WT TrpE or Q147K TrpE, was measured by the same assay. Each 500 μL reaction mixture contained 100 mM TEA-HCl (pH 9.0), 5 mM MgCl<sub>2</sub>, 4 mM 3-acetylpyridine adenine dinucleotide (APAD), 25 units of GDH, and 1.0 nM AS (same concentration used for both WT and Q147K reactions). The L-glutamine concentration was varied from 0.5 to 8.0 mM.

**HPLC Analysis.** The standard reaction mixture for HPLC analysis contained 100 mM bicine (pH 8.0) [AS-Gln reactions used 100 mM phosphate buffer (pH 7.0)], 5 mM chorismate, either 20 mM L-glutamine or 100 mM (NH<sub>4</sub>)<sub>2</sub>SO<sub>4</sub>, 5 mM MgCl<sub>2</sub>, and 20 μM enzyme(s).

After 3 h at room temperature, the samples were ultrafiltered to remove protein(s) and injected onto an Agilent 1100 HPLC system. Conditions for control reactions (no enzyme) were identical. A 5 μm Supelco Supelcosil (4.6 mm × 250 mm) C18 column was used to separate reaction mixtures. Mobile phase A consisted of a 5% acetic acid/water mixture; mobile phase B consisted of acetonitrile. Reaction mixtures were eluted isocratically at 95% A and 5% B for 15 min, followed by gradient elution in the following manner: 5 to 50% B from 15 to 18 min, 50% B from 18 to 25 min, and 50 to 5% B from 25 to 30 min. Two detectors were used. The first monitored absorbance at 280 nm. The second monitored fluorescence emission at 400 nm from excitation at 300 nm. The flow rate was 1.25 mL/min.

## RESULTS

**HPLC Analysis of Wild-Type and Mutant Enzyme-Catalyzed Reactions.** HPLC data are summarized in Tables 1–4. For each reaction condition, a nonenzymatic control reaction was performed. Peak area integration of each signal was corrected for the control sample. Adjusted peak areas were then converted to a concentration value by correlation with measured response factors. HPLC peak assignments were based on a comparison of retention times with those of authentic standards. Additional

Table 1: IS Product Distributions<sup>a</sup>

	NH <sub>4</sub> <sup>+</sup>		H <sub>2</sub> O	
	WT enzyme	K147Q enzyme	WT enzyme	K147Q enzyme
chorismate conversion (%)	59	48	38	3
isochorismate	41	4	100	100
ADIC	59	96		

<sup>a</sup>Reaction mixtures were incubated for 3 h at 25 °C and pH 8.0 prior to separation by RP-HPLC. Each product is reported as a fraction of all products formed. Chorismate conversion is the percentage of 5 mM chorismate enzymatically converted to products. All values were corrected for nonenzymatic controls run under identical conditions.

Table 2: SS Product Distributions<sup>a</sup>

	NH <sub>4</sub> <sup>+</sup>		H <sub>2</sub> O	
	WT enzyme	K147Q enzyme	WT enzyme	K147Q enzyme
chorismate conversion (%)	62	54	84	1.9
isochorismate	17	0.8	7	44
ADIC	42	77		
salicylate	40	1.2	93	56
anthranilate	1	21		

<sup>a</sup>Reaction mixtures were incubated for 3 h at 25 °C and pH 8.0 prior to separation by RP-HPLC. Each product is reported as a fraction of all products formed. Chorismate conversion is the percentage of 5 mM chorismate enzymatically converted to products. All values were corrected for nonenzymatic controls run under identical conditions.

chemical identification of ADC, ADIC, and isochorismate peaks has been reported previously (14, 16). Product distributions listed in Tables 1–4 reflect the fraction of total products formed by the specified enzyme.

*Removal of Lys147 Does Not Eliminate the Formation of Isochorismate by IS and SS.* If K147 is the base responsible for activating water as a nucleophile in the IS- and SS-catalyzed reactions, then the K → Q mutation is expected to render these enzymes unable to catalyze formation of isochorismate. Further, the ability to catalyze formation of ADIC and anthranilate by K → Q mutants of IS and SS, respectively, was expected to be unchanged relative to that of WT IS and SS if exogenous ammonia was supplied (Figure 2). HPLC chromatograms of reaction mixtures formed by WT IS and K147Q IS in the presence and absence of (NH<sub>4</sub>)<sub>2</sub>SO<sub>4</sub> are shown in Figure 4. Surprisingly, the K147Q mutant forms isochorismate despite losing its presumed catalytic base, at a rate reduced by ~25-fold relative to the WT rate. The HPLC data for WT IS reflect an equilibrium mixture; the isochorismate to chorismate concentration ratio is 0.56, which is identical to the  $K_{eq}$  reported by Liu et al. (23). As expected, K147Q IS retains the ability to catalyze formation of ADIC, and the HPLC data in Table 1 indicate that rates of formation of ADIC by WT and K147Q IS are similar.

HPLC chromatograms of product mixtures formed by WT SS and K147Q SS in the presence and absence of (NH<sub>4</sub>)<sub>2</sub>SO<sub>4</sub> are shown in Figure 5. Loss of the presumed catalytic base, Lys147, did not completely remove SS's ability to use water as a nucleophile, as evidenced by the presence of peaks due to isochorismate and salicylate in K147Q SS reaction mixtures. The data in Table 2

Table 3: AS Product Distributions<sup>a</sup>

	L-Gln		NH <sub>4</sub> <sup>+</sup>		H <sub>2</sub> O	
	WT enzyme	Q147K enzyme	WT enzyme	Q147K enzyme	WT enzyme	Q147K enzyme
	chorismate conversion (%)	100	0.3	100	30	0
isochorismate		8		0.6		21
ADIC				0.4		
salicylate		16		2		79
anthranilate	100	76	100	97		

<sup>a</sup>Reaction mixtures were incubated for 3 h at 25 °C and pH 8.0 prior to separation by RP-HPLC; L-Gln reactions were conducted at pH 7.0. Each product is reported as a fraction of all products formed. Chorismate conversion is the percentage of 5 mM chorismate enzymatically converted to products. All values were corrected for nonenzymatic controls run under identical conditions.

indicate that formation of these two products by K147Q SS occurs ~50-fold slower relative to WT SS.

The presence of peaks due to ADIC and anthranilate in Figure 5 indicates that both WT SS and K147Q SS employ ammonia as a nucleophile. In previous work with SS, Kerbarh et al. did not observe anthranilate in SS reaction mixtures that included NH<sub>4</sub>Cl (20). However, the inclusion of (NH<sub>4</sub>)<sub>2</sub>SO<sub>4</sub> in WT SS reaction mixtures inhibits its isochorismate pyruvate lyase activity. This is illustrated by the fact that the salicylate:isochorismate product ratio formed by WT SS when NH<sub>3</sub> is added is ~6-fold smaller than that observed in WT SS–H<sub>2</sub>O reactions (Table 2).

The data in Table 2 show interesting differences in the distribution of elimination products, i.e., anthranilate and salicylate, between WT SS and K147Q SS. An altered substrate preference for the pyruvate lyase activity is observed in reactions catalyzed by K147Q SS, relative to those catalyzed by WT SS. WT SS prefers isochorismate over ADIC as a substrate for its lyase activity. Despite a high concentration of ADIC (1.4 mM) available to WT SS, only 2% is converted to anthranilate. On the other hand, WT SS forms 1.2 mM salicylate, which represents a 20% conversion of 5 mM chorismate. The opposite trend is observed in K147Q SS reactions. Relative to WT SS, K147Q SS forms 18-fold more anthranilate. This equates to a 21% conversion of 2.1 mM ADIC. Conversely, if supplied with 2 mM isochorismate as the substrate in the absence of (NH<sub>4</sub>)<sub>2</sub>SO<sub>4</sub>, K147Q SS converts only 7% to salicylate.

*The Gln → Lys Mutation Does Not Engender High IS Activity in AS and ADCS.* In the simplest scenario, the Q → K mutation was expected to confer AS and K213A ADCS with salicylate synthase and isochorismate synthase activity, respectively. For ADCS, the K213A mutation was introduced to render it incapable of forming a Lys213–chorismate covalent intermediate (16). HPLC chromatograms of WT and mutant-catalyzed reactions, conducted in the absence of ammonia, are shown in Figure 6. The 100-fold expansion inset in the Q147K AS trace reveals the presence of a small peak due to isochorismate at 5.8 min and salicylate at 20.7 min (fluorescence signal displayed). Isochorismate was not detected in K213A/Q147K ADCS reaction mixtures.

The Q → K mutation was not anticipated to affect AS's ability to use ammonia as a nucleophile, since WT IS and WT SS, which possess an analogous lysine residue, display high ADIC synthase activity. L-Glutamine and (NH<sub>4</sub>)<sub>2</sub>SO<sub>4</sub> were both used as ammonia

Table 4: ADCS Product Distributions<sup>a</sup>

	PabA + L-Gln			PabA + NH <sub>4</sub> <sup>+</sup>			NH <sub>4</sub> <sup>+</sup>		
	WT enzyme	K213A enzyme	K213A/Q147K enzyme	WT enzyme	K213A enzyme	K213A/Q147K enzyme	WT enzyme	K213A enzyme	K213A/Q147K enzyme
chorismate conversion (%)	56	23	1.9	55	49	8.4	45	42	1.3
ADC	69	12		75	24	85	98	43	33
PABA <sup>b</sup>	31	45		25	50	15			
ADIC		43	100		26		2	57	67
isochorismate									

<sup>a</sup>Reaction mixtures were incubated for 3 h at 25 °C and pH 8.0 prior to separation by RP-HPLC. Each product is reported as a fraction of all products formed. Chorismate conversion is the percentage of 5 mM chorismate enzymatically converted to products. All values were corrected for nonenzymatic controls run under identical conditions. <sup>b</sup>PABA is formed by ADCL, which is present as a contaminant in PabA. Reactions were also conducted in the absence of an ammonia source; those results are not shown because no products were formed.

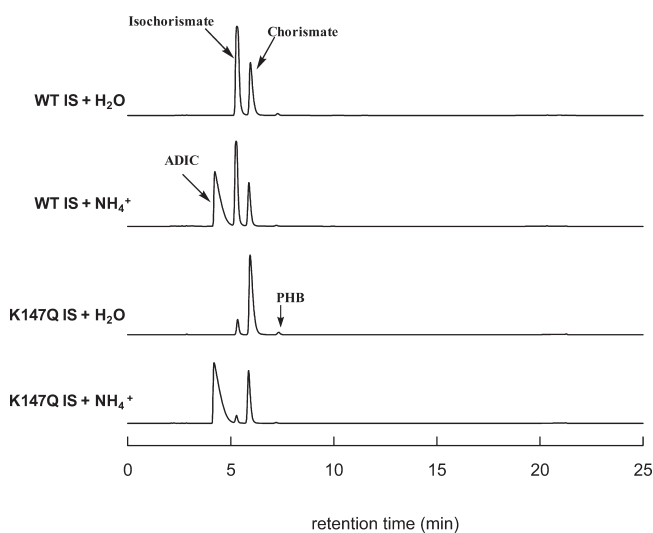


FIGURE 4: HPLC chromatograms of reactions catalyzed by IS or its mutant K147Q, in the presence and absence of 100 mM (NH<sub>4</sub>)<sub>2</sub>SO<sub>4</sub> (pH 8), with 5 mM chorismate as the substrate. PHB is *p*-hydroxybenzoate, a nonenzymatic decomposition product of chorismate.

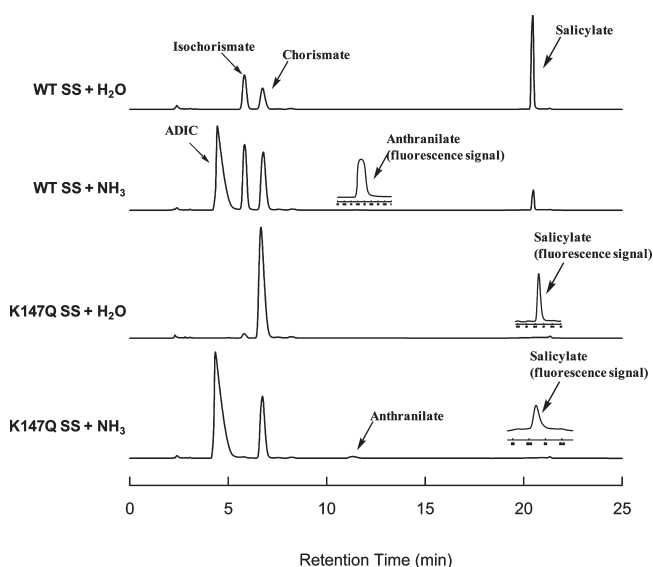


FIGURE 5: HPLC chromatograms of reactions catalyzed by SS and its Q147K mutant in the presence and absence of 100 mM (NH<sub>4</sub>)<sub>2</sub>SO<sub>4</sub> (pH 8). Chorismate (5 mM) was the substrate in each reaction. In cases of weak UV absorbance due to a low analyte concentration, fluorescence signals are included as insets, which are placed at the correct position on the time axis.

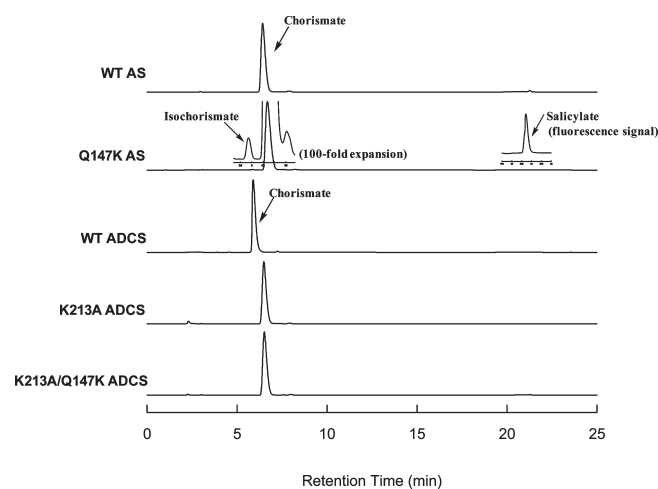


FIGURE 6: HPLC chromatograms of reactions catalyzed in the absence of an ammonia source by AS and its Q147K mutant and ADCS and its two mutants, K213A and K213A/Q147K. Chorismate (5 mM) was the substrate in each reaction. Insets (placed at the correct position on the time axis) in the Q147K AS trace emphasize the peaks due to isochorismate at 5.8 min and salicylate at 20.7 min. Small differences in chorismate retention times are due to slight variations in chromatographic conditions over the period of time during which the data were collected.

sources. Surprisingly, with L-glutamine, Q147K AS did not exhibit anthranilate synthase activity. However, using (NH<sub>4</sub>)<sub>2</sub>SO<sub>4</sub>, 29% of the WT activity was restored to Q147K AS, with anthranilate representing 97% of all products (see Table 3). This result indicates that exogenous ammonia has greater access to C2 of chorismate than the ammonia that is released from TrpG-mediated L-glutamine hydrolysis.

ADCS-catalyzed reactions were conducted under four different conditions: (1) PabA-Gln, (2) PabA-NH<sub>4</sub><sup>+</sup>, (3) NH<sub>4</sub><sup>+</sup>, and (4) H<sub>2</sub>O (Table 4). The results of the reactions conducted in the absence of an ammonia source are not listed in Table 4 because no products were formed. A small amount of activity is observed in ammonia-dependent reactions, regardless of the source [i.e., PabA with L-Gln or (NH<sub>4</sub>)<sub>2</sub>SO<sub>4</sub>]. Previous work has demonstrated that exogenous ammonia rescues the activity of K213A ADCS; in fact, when (NH<sub>4</sub>)<sub>2</sub>SO<sub>4</sub> is the ammonia source, the *k*<sub>cat</sub> values of WT and K213A ADCS are nearly identical (14). Therefore, the low activity of the double mutant is due to the Q147K mutation. With exogenous ammonia, ADC and ADIC were formed by K213A/Q147K ADCS at a rate 32-fold slower compared to that of K213A ADCS and 35-fold slower compared

Table 5: Amidotransferase Steady State Kinetic Data

	$K_{L-Gln}$ (mM)	$k_{cat}$ ( $s^{-1}$ )
WT ADCS	$0.52 \pm 0.11$	$0.67 \pm 0.05$
K213A/Q147K ADCS	$0.89 \pm 0.07$	$0.60 \pm 0.02$
WT AS	$2.5 \pm 0.4$	$138 \pm 9$
Q147K AS	$3.6 \pm 0.9$	$152 \pm 18$

to that of WT ADCS. The product distribution (ADC vs ADIC) in the double mutant is similar to that of K213A ADCS, which indicates that other catalytic steps are responsible for the slow turnover by K213A/Q147K ADCS. In other words, the nucleophilic addition steps may proceed at similar rates, but other processes, such as product release, may be slower for the double mutant, relative to K213A ADCS.

*Glutamine Amidotransferase Activity of TrpG and PabA.* AS is a heterotetramer, consisting of a TrpE–TrpG heterodimer. ADCS is a heterodimer of PabA and PabB subunits. To verify that the Q → K mutation in PabB or TrpE does not affect the glutamine amidotransferase activity of PabA or TrpG, respectively, production of free ammonia was monitored using glutamate dehydrogenase. PabA is a conditional amidotransferase; only when in complex with ADCS does it possess activity (22). Amidotransferase kinetic data, obtained with WT and mutant TrpE and PabB, confirm that neither TrpG nor PabA activity was affected by the mutation(s) in TrpE or PabB, respectively. These data are summarized in Table 5.

*AS, ADCS, IS, and SS Do Not Possess Chorismate Mutase and Prephenate Dehydratase Promiscuous Activities.* Before they were subjected to a second purification step, every enzyme under study here, including mutants, exhibited chorismate mutase (CM) promiscuous activity. Additionally, WT AS, Q147K AS, K213A ADCS, and K213A/Q147K ADCS exhibited prephenate dehydratase (PDT) activity as well. That is, they formed phenylpyruvate when supplied with prephenate as the substrate. However, these promiscuous activities were either completely removed or significantly reduced after the proteins were subjected to an additional orthogonal purification step (e.g., anion-exchange purification after nickel affinity purification). Representative HPLC data are shown for singly and doubly purified Q263K AS and WT SS in Figure 7. The peak at 21.8 min is due to phenylpyruvate. Phenylpyruvate is the acid-catalyzed decomposition product of prephenate. HPLC separations were performed at pH 4. Therefore, phenylpyruvate appears in the HPLC chromatogram regardless of whether the enzymes possess PDT promiscuous activity in addition to CM promiscuous activity.

## DISCUSSION

The survival of bacteria, plants, fungi, and apicomplexan parasites depends on the activity of several chorismate-utilizing enzymes, which catalyze the first committed step in the biosynthesis of aromatic amino acids, folate, siderophores, quinones, and others (1, 2). These enzymes are attractive targets for antimicrobial drugs, but they have not yet been exploited for this purpose. Understanding more fully their catalytic mechanisms may assist drug discovery efforts. AS, ADCS, IS, and SS each catalyze a nucleophilic substitution reaction, and new information for characterizing this step in catalysis is presented.

An important finding of this work is that AS, ADCS, IS, and SS do not possess CM promiscuous activity. This contradicts several previous studies (20, 24, 25). CM activity was observed in

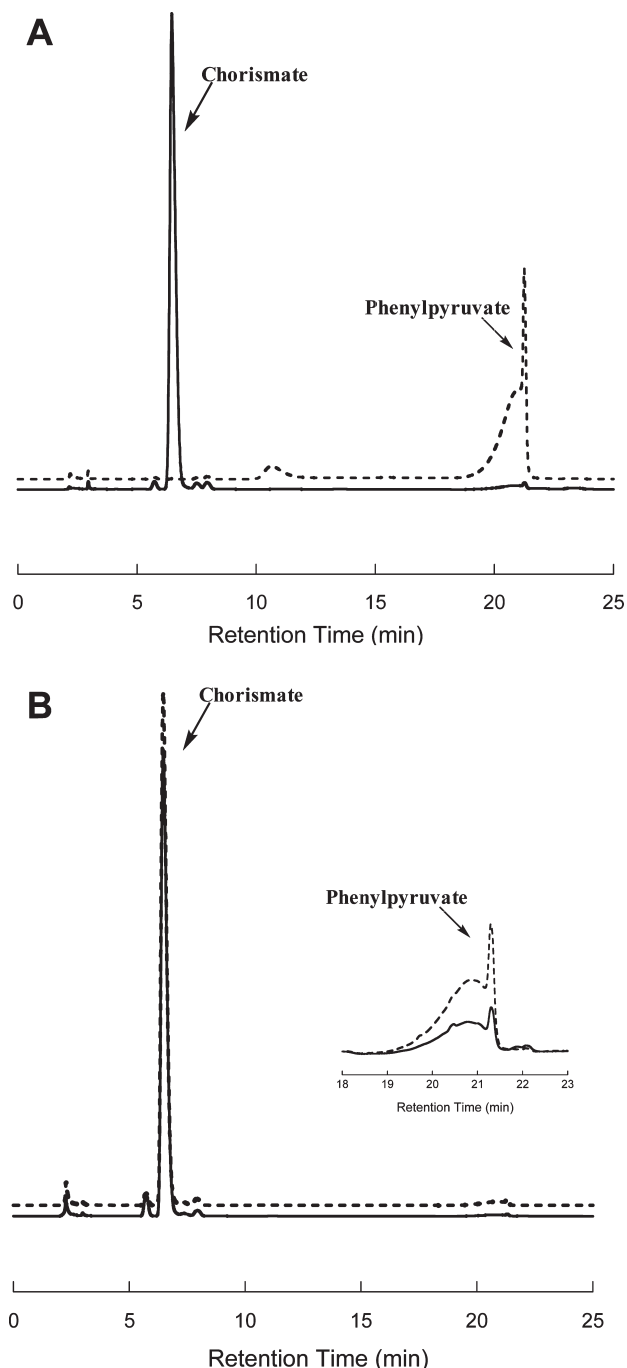


FIGURE 7: HPLC traces of singly (---) and doubly (—) purified SS (A) and Q147K AS (B). Chorismate mutase activity, indicated by the presence of phenylpyruvate, is significantly reduced after a second purification.

singly purified proteins, but it was abolished or significantly reduced in doubly purified proteins. Therefore, the observed CM activity, originally thought to be a promiscuous activity of ADCS, AS, IS, and SS, is due to authentic chorismate mutase present in singly purified proteins that were expressed by an *E. coli* lab strain [BL21(DE3)]. The *E. coli* chorismate mutase is a bifunctional enzyme, possessing mutase and prephenate dehydratase activities, with a  $k_{cat}$  of  $50 s^{-1}$  (26). Such an enzyme could generate detectable product after 3 h even if present at nanomolar to picomolar concentrations. Indeed, on the basis of this  $k_{cat}$  value and the concentration of phenylpyruvate measured by HPLC, the CM concentration in the AS preparation was calculated to be 9 nM, which translates to a 0.05% contamination. The smallest

concentration of CM present in any protein sample was 10 pM. The four singly purified proteins originally thought to possess PDT promiscuous activity (WT AS, Q263K AS, K213A ADCS, and K213A/Q147K ADCS) in addition to CM promiscuous activity all contained nanomolar levels of CM. Removal of the contaminating *E. coli* CM protein by secondary purification schemes facilitated efforts to investigate nucleophile specificity in AS, ADCS, IS, and SS. In some mutant enzymes, nearly 100% of chorismate was converted to phenylpyruvate. Thus, the removal of the competing CM activity allowed detection of mutant enzyme-catalyzed reaction products by HPLC.

The retention of cognate activity in K147Q IS and K147Q SS activity was a surprising result that contrasts with earlier reports (see Figures 4 and 5) (9, 20, 24). It is unlikely that this activity is due to a contamination of WT IS and SS in the mutant preparations. After each mutant had been subjected to an additional purification step, the isochorismate synthase activity increased slightly. Furthermore, the HPLC data in Figure 6 indicate that the Q → K mutation enables AS to activate water as a nucleophile, albeit to a small extent. With a calculated HPLC detection limit of ~0.3 μM for isochorismate, introduction of Lys147 into AS enhanced its ability to activate water at pH 8 by at least 100-fold compared to that of WT. The WT reactions showed no detectable amounts of isochorismate or salicylate at pH 7, 8, or 9, while the Q → K mutant gave 10- and 2-fold increases on going from pH 7 to 8 and from pH 8 to 9, respectively (data not shown). These changes as a function of pH are best interpreted as deprotonation of a general base catalyst in the active site (assumed here to be the introduced Lys); they are inconsistent with hydroxide acting as a nucleophile since only a 2-fold increase is observed on going from pH 8 to 9, while a 10-fold increase is observed on going from pH 7 to 8.

While the results described above qualitatively agree with Kolappan's assertion that Lys147 is the catalytic base, they strongly suggest that Lys147 is not the sole determinant of water activation as a nucleophile given the high activity remaining in the K → Q mutants. The results also suggest that in IS and SS a different residue may act as a general base catalyst in the absence of Lys147; however, its identification is not possible on the basis of the available data. An alternative explanation is that Lys147 increases the reactivity of water 25-, 50-, and 100-fold in IS, SS, and Q147K AS, respectively.

The failure to introduce IS activity into ADCS with a Q → K mutation and the smaller than expected amount of SS activity imparted to AS by the same mutation prompted a close inspection of multiple-sequence (54 total) and structural (6 total) alignments of AS, ADCS, IS, and SS. This analysis revealed two additional structural features that correlate with the ability to activate water as a nucleophile: (1) the presence of two hydrogen bond acceptors, one on either side of Lys147, to position appropriately the ε-amino group toward C2 of chorismate and (2) the presence of either leucine or isoleucine at position 244 instead of methionine (Figure 8), which occupies the analogous position in all AS and ADCS sequences.

The correct orientation of Lys147 with respect to C2 of chorismate is critical since it is expected to act as a general base (i.e., removing a proton from water simultaneous with the O attacking C2). This is achieved via two hydrogen bonds, one on each side of the ε-amino group. In the Irp9 SS structure, these hydrogen bond acceptors are Ser245 and the backbone carbonyl of Glu241 (Figure 8A). Ser245 is conserved in all SS sequences, while leucine, isoleucine, and valine exist at the homologous position

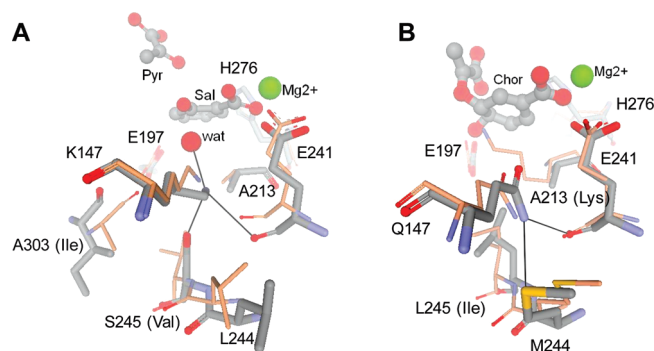


FIGURE 8: SS, IS, AS, and ADCS active sites. EntC IS residue numbering is used throughout. (A) Overlay of Irp9 SS residues (gray carbons) and MenF IS (peach carbons). IS residues differing from SS are indicated in parentheses. Irp9 SS crystallized in the presence of its reaction products salicylate and pyruvate. Lys147 is the presumed catalytic base that activates water as a nucleophile. (B) AS residues (gray carbons) and the analogous ADCS residues (peach carbons). Residues unique to ADCS are indicated in parentheses. Chorismate was superimposed onto the benzoate molecule present in the AS crystal structure.

in AS, ADCS, and IS sequences, respectively. In the MenF IS structure, the backbone carbonyl of Ala303, which is ~3 Å from Lys147, is positioned to replace Ser245 as the hydrogen bond acceptor. Analogous hydrogen bond interactions are not available to position correctly the introduced lysine residue in Q → K AS and ADCS mutants. This may partly explain their low IS activity. Each IS and SS sequence contains either leucine or isoleucine at position 244. Leu244 exists in the two SS structures and one IS structure available. Leu244 may also assist the proper positioning of Lys147 in IS and SS; from the structures, it appears to make van der Waals interactions with the methylene carbons of the Lys147 side chain.

The conserved methionine residue at position 244 in AS and ADCS sequences is related to their specificity for ammonia as a nucleophile. As shown in Figure 8B, a hydrogen bond between the methionine sulfur atom and the Gln147 amide side chain is possible. This interaction keeps the side chain of Gln147 pointed toward Met244. When Gln147 is held in such a position, it creates an appropriately sized cavity through which ammonia, arriving via the tunnel from the TrpG active site, may access C2 of chorismate.

A pairwise positional correlation analysis of 54 AS, ADCS, IS, and SS sequences, performed using the online CRASP program (27), corroborated the supposition that the identity of residue 244 is a critical component of the nucleophile specificity displayed by these enzymes. In the CRASP analysis, the “energy of transfer from water to ethanol” parameter was chosen with a variability threshold of 2 and a significance output value of 99.99%. Under these parameters, Lys147 was found to be correlated to Leu244 with a linear correlation value of 0.98. Leu244 corresponds to methionine in all AS and ADCS sequences.

Kerbarh et al. suggested that Lys147 plays a dual role in SS and IS nucleophile specificity, both as an activator of water and, via steric and/or electronic forces, as a repressor of ammonia as a nucleophile (20). However, the formation of ADIC by WT IS, WT SS, and K213A/Q147K ADCS and the formation of anthranilate by Q147K AS argue against this assertion. Since intracellular concentrations of ammonia are generally low, IS and SS apparently have not developed a means of discriminating against this nucleophile.

The presence of an amidotransferase subunit is the most important factor that determines which enzymes will employ

ammonia as a nucleophile. The ~450-fold reduction of cognate activity in Q147K AS when L-glutamine is the source of ammonia indicates that the identity of residue 147 is important insofar as it must not block the access of ammonia to the TrpE active site. An ~30-fold reduction in K213A/Q211K ADCS cognate activity was observed under L-Gln conditions. This suggests that the PabA–PabB interface, and, hence, the ammonia tunnel that is believed to connect the two active sites, is oriented slightly differently than the TrpG–TrpE interface observed in the AS crystal structure (5). The ADCS crystal structure was not determined in the presence of PabA (7); therefore, the precise arrangement of PabA and PabB subunits is unknown.

The data in Tables 2 and 3 suggest that SS pyruvate lyase activity is partially controlled by Lys147. In WT SS–NH<sub>3</sub> and K147Q SS–NH<sub>3</sub> reactions, significant build-up of ADIC was observed (Figure 5). Notably, ADIC does not accumulate in WT AS reactions, and 96% of ADIC is converted to anthranilate by Q147K AS when (NH<sub>4</sub>)<sub>2</sub>SO<sub>4</sub> is the ammonia source. Morollo and Bauerle demonstrated that ADIC is an intermediate in the AS reaction (28). If Lys147 were the sole determinant of reaction specificity (i.e., formation of anthranilate vs salicylate), then a K → Q mutation would render SS equivalent to AS, since each possesses pyruvate lyase activity. However, WT SS forms little anthranilate, despite high concentrations of ADIC in the reaction mixture. On the other hand, anthranilate represents 97% of all products formed in Q263K AS–NH<sub>3</sub> reactions. These contrasting results suggest that SS reaction specificity is controlled by factors beyond the selection of water as a nucleophile. The improved ability of K147Q SS to aromatize ADIC and a weakened ability to aromatize isochorismate (relative to WT SS) additionally support this notion. Future efforts will be aimed at uncovering the forces that dictate elimination specificity among AS, SS, ADCS, and IS.

## REFERENCES

- Roberts, F., Roberts, C. W., Johnson, J. J., Kyle, D. E., Krell, T., Coggins, J. R., Coombs, G. H., Milhous, W. K., Tzipori, S., Ferguson, D. J., Chakrabarti, D., and McLeod, R. (1998) Evidence for the shikimate pathway in apicomplexan parasites. *Nature* 393, 801–805.
- Dosselaere, F., and Vanderaeyden, J. (2001) A metabolic node in action: Chorismate-utilizing enzymes in microorganisms. *Crit. Rev. Microbiol.* 27, 75–131.
- Mavrodi, D. V., Ksenzenko, V. N., Bonsall, R. F., Cook, R. J., Boronin, A. M., and Thomashow, L. S. (1998) A seven-gene locus for synthesis of phenazine-1-carboxylic acid by *Pseudomonas fluorescens* 2-79. *J. Bacteriol.* 180, 2541–2548.
- Kerbarh, O., Chirgadze, D. Y., Blundell, T. L., and Abell, C. (2006) Crystal structures of *Yersinia enterocolitica* salicylate synthase and its complex with the reaction products salicylate and pyruvate. *J. Mol. Biol.* 357, 524–534.
- Morollo, A. A., and Eck, M. J. (2001) Structure of the cooperative allosteric anthranilate synthase from *Salmonella typhimurium*. *Nat. Struct. Biol.* 8, 243–247.
- Knochel, T., Ivens, A., Hester, G., Gonzalez, A., Bauerle, R., Wilmanns, M., Kirschner, K., and Jansonius, J. N. (1999) The crystal structure of anthranilate synthase from *Sulfolobus solfataricus*: Functional implications. *Proc. Natl. Acad. Sci. U.S.A.* 96, 9479–9484.
- Parsons, J. F., Jensen, P. Y., Pachikara, A. S., Howard, A. J., Eisenstein, E., and Ladner, J. E. (2002) Structure of *Escherichia coli* aminodeoxychorismate synthase: Architectural conservation and diversity in chorismate-utilizing enzymes. *Biochemistry* 41, 2198–2208.
- Spraggon, G., Kim, C., Nguyen-Huu, X., Yee, M. C., Yanofsky, C., and Mills, S. E. (2001) The structures of anthranilate synthase of *Serratia marcescens* crystallized in the presence of (i) its substrates, chorismate and glutamine, and a product, glutamate, and (ii) its end-product inhibitor, L-tryptophan. *Proc. Natl. Acad. Sci. U.S.A.* 98, 6021–6026.
- Kolappan, S., Zwahlen, J., Zhou, R., Truglio, J. J., Tonge, P. J., and Kisker, C. (2007) Lysine 190 is the catalytic base in MenF, the menaquinone-specific isochorismate synthase from *Escherichia coli*: Implications for an enzyme family. *Biochemistry* 46, 946–953.
- Harrison, A. J., Yu, M., Gardenborg, T., Middleditch, M., Ramsay, R. J., Baker, E. N., and Lott, J. S. (2006) The structure of MbtI from *Mycobacterium tuberculosis*, the first enzyme in the biosynthesis of the siderophore mycobactin, reveals it to be a salicylate synthase. *J. Bacteriol.* 188, 6081–6091.
- Parsons, J. F., Shi, K. M., and Ladner, J. E. (2008) Structure of isochorismate synthase in complex with magnesium. *Acta Crystallogr. D* 64, 607–610.
- Walsh, C. T., Liu, J., Rusnak, F., and Sakaitani, M. (1990) Molecular Studies on Enzymes in Chorismate Metabolism and the Enterobactin Biosynthetic-Pathway. *Chem. Rev.* 90, 1105–1129.
- Kozlowski, M. C., Tom, N. J., Seto, C. T., Seifler, A. M., and Bartlett, P. A. (1995) Chorismate-utilizing enzymes isochorismate synthase, anthranilate synthase, and *p*-aminobenzoate synthase: Mechanistic insight through inhibitor design. *J. Am. Chem. Soc.* 117, 2128–2140.
- He, Z., Stigers Lavoie, K. D., Bartlett, P. A., and Toney, M. D. (2004) Conservation of mechanism in three chorismate-utilizing enzymes. *J. Am. Chem. Soc.* 126, 2378–2385.
- Bulloch, E. M. M., and Abell, C. (2005) Detection of covalent intermediates formed in the reaction of 4-amino-4-deoxychorismate synthase. *ChemBioChem* 6, 832.
- He, Z., and Toney, M. D. (2006) Direct detection and kinetic analysis of covalent intermediate formation in the 4-amino-4-deoxychorismate synthase catalyzed reaction. *Biochemistry* 45, 5019–5028.
- Raushel, F. M., Thoden, J. B., and Holden, H. M. (2003) Enzymes with molecular tunnels. *Acc. Chem. Res.* 36, 539–548.
- Huang, X. Y., Holden, H. M., and Raushel, F. M. (2001) Channeling of substrates and intermediates in enzyme-catalyzed reactions. *Annu. Rev. Biochem.* 70, 149–180.
- Bauerle, R., Hess, J., and French, S. (1987) Anthranilate synthase-anthranilate phosphoribosyltransferase complex and subunits of *Salmonella typhimurium*. *Methods Enzymol.* 142, 366–386.
- Kerbarh, O., Ciulli, A., Chirgadze, D. Y., Blundell, T. L., and Abell, C. (2007) Nucleophile selectivity of chorismate-utilizing enzymes. *ChemBioChem* 8, 622–624.
- Grisostomi, C., Kast, P., Pulido, R., Huynh, J., and Hilvert, D. (1997) Efficient *In Vivo* Synthesis and Rapid Purification of Chorismic Acid Using an Engineered *Escherichia coli* Strain. *Bioorg. Chem.* 25, 297–305.
- Roux, B., and Walsh, C. T. (1992) *p*-Aminobenzoate synthesis in *Escherichia coli*: Kinetic and mechanistic characterization of the amidotransferase PabA. *Biochemistry* 31, 6904–6910.
- Liu, J., Quinn, N., Berchtold, G. A., and Walsh, C. T. (1990) Overexpression, purification, and characterization of isochorismate synthase (EntC), the first enzyme involved in the biosynthesis of enterobactin from chorismate. *Biochemistry* 29, 1417–1425.
- Zwahlen, J., Kolappan, S., Zhou, R., Kisker, C., and Tonge, P. J. (2007) Structure and mechanism of MbtI, the salicylate synthase from *Mycobacterium tuberculosis*. *Biochemistry* 46, 954–964.
- Zhou, R., Zwahlen, J., Subramaniapillar, K., Kisker, C., and Tonge, P. (2006) Comparative structural and biochemical studies of chorismate binding enzymes, MenF, EntC and MbtI. *FASEB J.* 20, A463.
- Lee, A., Stewart, J. D., Clardy, J., and Ganem, B. (1995) New insight into the catalytic mechanism of chorismate mutases from structural studies. *Chem. Biol.* 2, 195–203.
- Afonnikov, D. A., Oschepkov, D. Yu., and Kolchanov, N. A. (2001) Detection of conserved physico-chemical characteristics of proteins by analyzing clusters of positions with co-ordinated substitutions. *Bioinformatics* 17 (11), 1035–1046.
- Morollo, A. A., and Bauerle, R. (1993) Characterization of composite aminodeoxyisochorismate synthase and aminodeoxyisochorismate lyase activities of anthranilate synthase. *Proc. Natl. Acad. Sci. U.S.A.* 90, 9983–9987.